Low temperature luminescence from the near surface region of Nd:YAG

2001 J. Phys.: Condens. Matter 13 2497

(http://iopscience.iop.org/0953-8984/13/11/308)

INSTITUTE OF PHYSICS PUBLISHING JOURNAL OF PHYSICS: CONDENSED MATTER

J. Phys.: Condens. Matter **13** (2001) 2497–2515 www.iop.org/Journals/cm PII: S0953-8984(01)20188-X

Low temperature luminescence from the near surface region of Nd:YAG

M Maghrabi[1], P D Townsend[2] and G Vazquez[2,3]

[1] CPES, University of Sussex, Brighton BN1 9QH, UK
[2] EIT, University of Sussex, Brighton BN1 9QH, UK
[3] Centro de Investigaciones en Óptica, Lomas del Bosque 115, Lomas del Campestre León, Guanajuato, 37150 México

E-mail: p.d.townsend@sussex.ac.uk

Received 12 February 2001

Abstract

Luminescence offers a sensitive probe of the quality of Nd:YAG laser material both in the bulk and, via cathodoluminescence, in the near surface layers. The spectral signals are primarily from the Nd dopants, but the thermoluminescence spectra reveal traces of impurities such as Tb, Cr and Mn. Control of the electron energy of the cathodoluminescence demonstrates that the outer few micron layers differ significantly in luminescence response from the bulk crystal. The cathodoluminescence signals are influenced by near surface dislocations and solvents from cleaning treatments. The effects are often apparent as discontinuities in the Nd signal intensities at temperatures which match the solid–liquid or liquid–gas phase transitions of contaminants. Additionally there is strong evidence for the inclusion of carbon dioxide, in the form of nanoparticles. At 202 K, the CO_2 sublimation temperature, the Nd line intensities change discretely and there are wavelength shifts for some of the emission lines consistent with pressure driven changes in the lattice parameter. Data for x-ray lattice parameters identify a complex and sudden change and expansion of the lattice in this temperature region. The luminescence methods used suggest identification of impurities and gaseous inclusions can be exploited in other insulator materials and examples are cited.

1. Introduction

Neodymium doped yttrium aluminium garnet (Nd:YAG, $Y_3Al_5O_{12}$) has successfully been used as an active laser medium for more than 30 years. It can be grown in the form of large boules from which are cut laser rods of relatively good optical quality, high mechanical strength and high thermal conductivity. Nevertheless the growth conditions introduce some stresses, so the boule centre is avoided and the presence of dislocations reduces the laser performance [1]. There is evidence of surface changes with time and surface polishing degrades the system by introducing a high density of surface dislocations [2]. Surface dislocations and related damage

features are particularly problematic in the production of Nd:YAG waveguide lasers since the waveguides are immediately adjacent to the surface. Recent work has focused on the possibility of packaging the laser crystal in the form of a thin layer. Here again the main problem in doing so is to obtain a surface free from dislocations and scratches caused by cutting and polishing, as the luminescence efficiency and laser performance are strongly dependent on the dislocation density. Usually the modified surface is poorer in quality than that of the bulk material and therefore there is a need to improve the surface quality. Surface quality is similarly important for waveguides made by epitaxial growth on a polished substrate. Results aimed at improving surface perfection are very promising and indicate that the surface, and near surface, regions can be greatly enhanced by ion beam amorphization followed by chemical etching [2–5]. The process strips off the region containing the polishing damage. Assessment of the improved surface quality has been achieved using three different techniques namely, cathodoluminescence (CL), scanning electron microscopy (SEM) and surface second harmonic generation (SSHG).

The trivalent Nd^{3+} ions enter the YAG lattice substitutionaly on the sites normally occupied by the trivalent yttrium Y^{3+}, consequently the charge balance is attained without the need for charge compensation. Despite this advantage, the colour centre studies in this material are rather few and the luminescence studies in the UV–visible region are limited. There are several possible non-equivalent lattice sites and a consequence of this is that the structures of the trapping centres in YAG are still not well identified either for luminescence or thermoluminescence (TL). Although the concept of radiationless energy transfer between traps and emission sites is widely accepted [6–9], the detailed structure of the lattice defects is still controversial. The various models that have been proposed indicate the diversity of opinion. Examples include those by Cermak and Linka [10], Mori [11], Bernhardt [12] and Hayes *et al* [6]. The electron beams used in CL typically only excite the material to a depth of say 1 micron (e.g. for energies of $\sim$20 keV) thus spectral analysis of luminescence from CL, and also from TL following the electron irradiation, offers data on the imperfections and quality of the near surface layers. Such signals can be contrasted with bulk effects. Typically these are recorded during x-ray irradiation (radioluminescence, RL) and/or during the subsequent TL measurements. The present work was stimulated by observations of unusual behaviour recorded during CL measurements whilst heating from 25 K. In particular the data showed discontinuous changes in emission intensity, and/or spectra. Such features have not previously been reported but similar anomalies were also seen in a set of parallel luminescence studies from other oxide insulator materials [13, 14] (no such effects have been noted so far for halide samples).

2. Experiment

Nd:YAG laser quality crystals were obtained from the Roditi Corporation. Czochralski growth, using low pulling and sample rotation rates, has been used to minimize the dislocation density and strain, and to attempt to offer homogeneity in the Nd concentration. Despite this approach providing good laser quality material there is still evidence for facets and growth striations. These are always major problems in growing YAG crystals, and are the main cause of impurity segregation and point defects in YAG [15–18]. Excitation and spectral measurements were carried out on a high sensitivity wavelength multiplexed system with temperature control either from 20 to 300 K, or above room temperature from 20 to 400 °C. The equipment has *in situ* facilities for both electron and x-ray radiation, and so can be used for conventional CL and RL at a fixed temperature. Alternatively the CL and RL can be recorded during a controlled linear rate of temperature change. Linear heating or cooling are possible. Equally, an irradiated sample can be monitored by subsequent thermoluminescence. The system has been described in many earlier articles [19, 20]. The key features are that it offers very high recording sensitivity (via

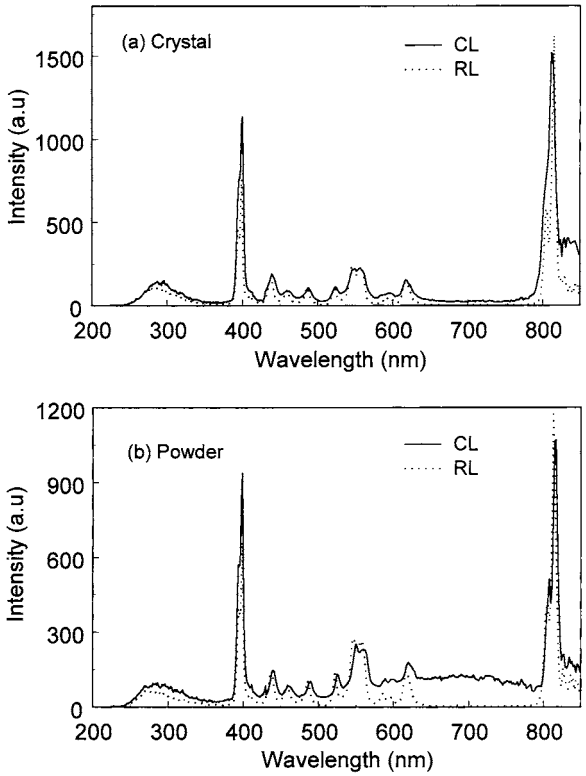

Figure 1. RL and CL spectra of Nd:YAG at 25 K. (a) Crystal sample, (b) powder.

$f/2$ optics) and spectra which are taken simultaneously at all wavelengths. Therefore during heating or cooling there are none of the uncertainties in observing spectral changes as a function of temperature which are inherent in scanning monochromator recording.

The Nd:YAG crystals show an extremely bright signal from the bulk material upon x-ray irradiation, whereas the surface studies with CL activate only a small volume of material as a result of the limited electron penetration, and so offer weak signals. Variations in spectra, temperature dependence and component TL peaks occur with changes in electron energy and these CL features will be discussed later. The CL surface signals are sensitive to the methods of preparation and in particular examples of data resulting from chemical cleaning treatments, including ethanol or hydrochloric acid (HCl), were noted. Some initial attempts to resolve depth dependent signal changes were explored by varying the energy of the incident electrons. The incident energy was varied from 25 to 5 keV in steps of 5 keV (i.e. the maximum electron penetration is thus $\sim$1 micron). Finally, the CL spectra from Nd:YAG crystals and powder were compared.

3. Results and comments

3.1. RL and CL spectra

Figure 1(a) compares the RL and CL spectra of Nd:YAG at 25 K (i.e. signals which are primarily from the near surface are seen in CL and bulk signals dominate the RL spectra). The narrow line signals are primarily from Nd transitions although there are overlapping broad

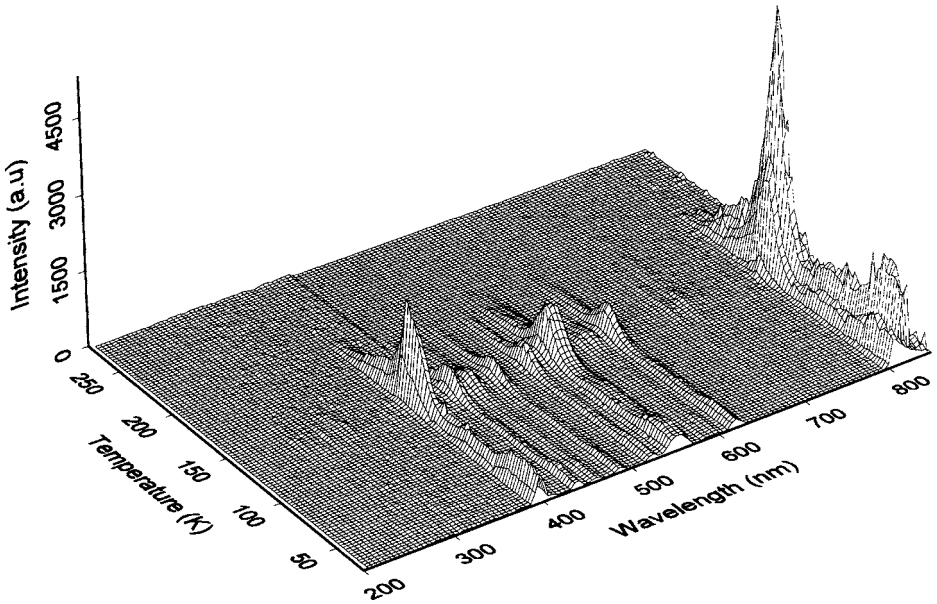

Figure 2. Low temperature TL spectrum of Nd:YAG after x-ray irradiation.

band intrinsic emission features in the ultra-violet between 250 and 350 nm. There are both relative intensity changes between the lines under these alternative conditions of excitation and some spectral shifts between the RL (bulk) and CL (near surface) signals. In general the RL lines are sharper than those seen by CL. Such line broadening is to be expected as there will be variations in site geometry caused by the polishing which will have introduced dislocations and distortions in a damaged surface layer. In order to emphasize surface effects signals were recorded from a crystal which had been ground into a powder form (figure 1(b)). For powder sizes of a few micron dimensions the material may be considered as being equivalent to $\sim$100% 'surface' material. Figures 1(a) and 1(b) underline that there are shifts in the peak emission wavelengths, and different structure in the broad UV bands. For the powder material there is a greatly enhanced emission from 550 to 800 nm. The details of the spectra change with temperature, and at room temperature the crystalline signals provide almost no UV signals in RL; however there are some UV signals near 300 nm generated during CL.

3.2. Thermoluminescence

The low temperature thermoluminescence of Nd:YAG after x-ray or electron irradiation are very similar and data from an x-ray example are shown in figure 2. There are minor spectral differences in the relative intensity and the temperature spread of the main glow peak. As expected for a distorted surface region, in which there are likely to be variations in detailed site symmetry, the TL glow peaks are wider in electron irradiated samples. The main glow peak occurs near 140 K together with two smaller ones around 40 and 90 K. The glow curves resemble those reported in earlier publications, although they differ in detail [8, 21]. In the UV region the intrinsic emission, seen during RL or CL, is almost completely suppressed. Instead there are three separate Nd line signals. These are emitting at very low intensity (i.e. not visible in this presentation). These UV Nd transitions were obscured in RL and CL by the strong intrinsic emission bands.

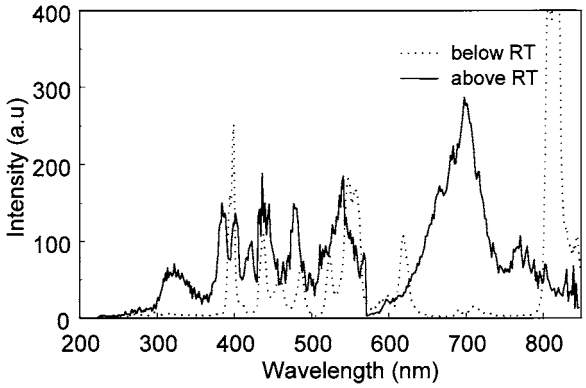

Figure 3. Wavelength slices which compare the emission from TL below and above room temperature.

Above room temperature the RL and CL generate the same pattern of Nd line emissions as at low temperature. This is not so for thermoluminescence and, surprisingly, TL above room temperature reveals very different glow spectra (figure 3). This again has characteristic rare earth line features, but the lines match to transitions from trace impurities of Tb (as listed in table 1). A similar situation has been encountered by Niklas [8]. Such differences emphasize how the CL, RL and TL methods offer complementary information arising from alternative methods of luminescence generation.

Table 1. The wavelengths of transitions between states for Tb ions.

Initial state	Final state	Emitted light (nm)
$^5D_3$	$^7F_6$	380
$^5D_3$	$^7F_5$	420
$^5D_3$	$^7F_4$	440
$^5D_4$	$^7F_6$	480
$^5D_4$	$^7F_5$	540

The broad band between 600 and 750 nm can not be attributed to either Tb or Nd ions. This implies there is at least a third impurity participating in the TL above room temperature. Two possible candidates are Mn and Cr and similar spectra have been cited both for Cr dopants [8, 22], or in more detail, for Mn doped crystals [12, 23] where the emissions at 680 and 710 nm were attributed to Mn^{4+} and those at 595 nm to Mn^{2+}. There are minor differences in glow peak temperatures as a function of wavelength, which may indicate that both impurities are present. In an attempt to clarify the situation, data were collected from a sample of Cr:YAG. In this case there was no evidence of Tb impurities during TL; however the broad emission band near 700 nm was again apparent. Whilst this is in agreement with the view that the Cr is a probable source of the emission signal the intensity did not increase in proportion to the high Cr content. In fact, although the Cr content had been raised, the intensity, and signal to noise, from the band was reduced. Such concentration quenching is not uncommon but it may indicate that for the Cr doping there is clustering of the impurity ions to minimize lattice strain (as in ruby, Al_2O_3:Cr). This leads to a consequent reduction in luminescent intensity which arises from isolated ions. Indeed the distortions of Cr^{4+} in Ga^{3+} lattice sites of YAG have recently been discussed in similar terms [24].

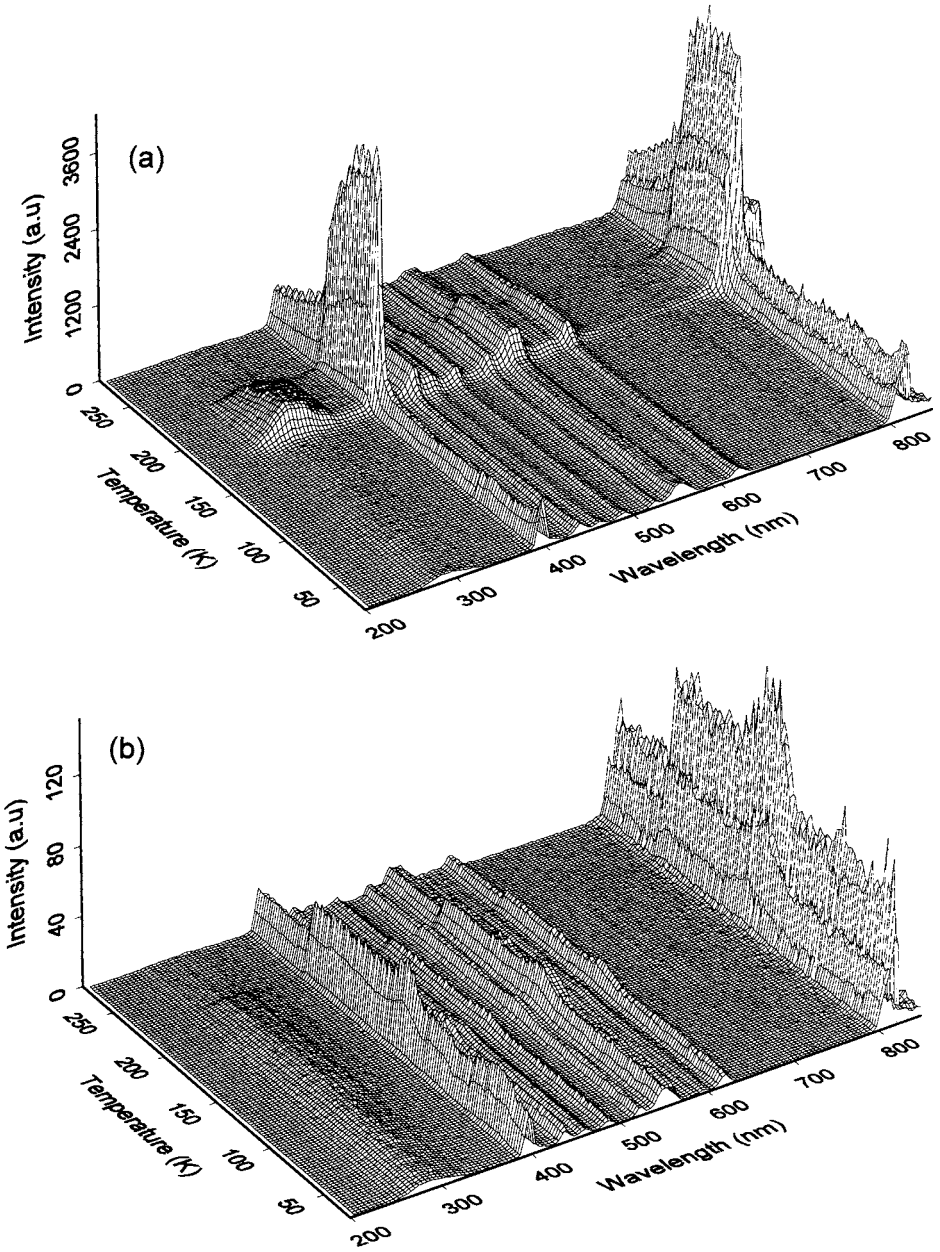

Figure 4. Isometric plots of (a) cathodo-thermoluminescence (CLTL), (b) radio-thermoluminescence (RLTL).

3.3. RL and CL during heating or cooling

In a dynamic experiment, where there is continuous excitation during heating, the signals are likely to demonstrate a combination of normal excited luminescence and thermoluminescence. Additionally, with continuous repopulation of trapping states there may be TL features which are absent in conventional TL. The radio- and cathodo-thermoluminescence (RLTL and CLTL)

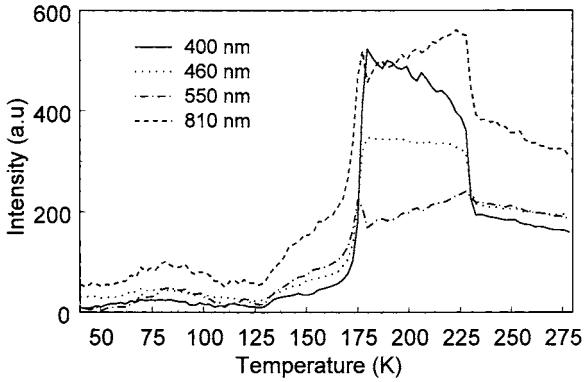

Figure 5. Temperature dependence of selected wavelengths of Nd:YAG after immersion in ethanol.

spectra below room temperature indeed show a mixture of steady state luminescence plus some TL type signals. However the surface and bulk dominated signals from CLTL and RLTL have very distinct features, as contrasted by figures 4(a) and 4(b). For RLTL weak glow peaks are superposed on the background RL signals, but for CL such TL components are less obvious or absent. An unusual feature in both cases is a sharp drop in intensity near 220 K. This is most obvious for CLTL. Additionally there is a major and sudden intensity increase near 175 K. Note that neither feature has the shape associated with a standard TL component (i.e. these are not broad glow peaks superposed on a continuous background). The scale of the discontinuities in intensity vary for the different Nd lines. For example in the RLTL case the intrinsic broad band UV signal is virtually quenched above the ∼220 K step, whereas the Nd lines persist at a reduced level. For the CLTL case the UV signals are only significant in a limited range, as are signals at the longest wavelength signal shown here (∼830 nm). Note also that detailed contour maps indicate minor wavelength movements can be resolved for the signals near 400 and 800 nm (even with the relatively low spectral resolution of this spectrometer). Temperature dependencies of such changes are typified by figure 5 (as commented on later).

One possible reason for such rapid intensity changes in luminescence intensity is the presence of a phase transition [25] since there will be major changes in luminescence efficiency associated with differences in phase. Whilst phase changes might arise from an intrinsic lattice relaxation, as clearly exemplified by luminescence data for ammonium bromide [25], or potassium niobate [26], no such structural changes are expected for Nd:YAG. However phase instabilities have been considered in a study of $YAlO_3$:Nd [27]. The present authors are conducting parallel work with several other oxide materials, such as bismuth germanate or MgO. In each case there are strong suggestions that discontinuities in luminescence intensity and emission wavelength can arise from the presence of impurity phases. For example micro-bubbles of trapped CO_2 would induce a major pressure change when the CO_2 material sublimes near 202 K, resulting in line shifts and alterations in luminescence efficiency. Equally the presence of solvents trapped in the near surface layer could provide either volume (i.e. pressure) effects and/or electronic variations between activation, or quenching, of luminescence when the additive undergoes changes in phase. Again a clearly documented example exists for a phase change of a fullerene that was monitored by the luminescence intensity derived from traces of solvents [20]. To test this impurity phase transition model Nd:YAG samples were variously washed, or soaked, in cleaning or solvent materials such as acetone, ethanol and hydrochloric acid. These were selected on the basis of known phase transitions of the solvents (e.g. ethanol melts at 156 K) or compounds that might form within the YAG lattice, particularly where

reactivity with surface dislocations is feasible. Examples of compounds formed by chemical reactions include examples such as COS or Cl_2, where boiling points are cited at 223 and 238 K. Similarly, compounds of the type $C_\alpha O_\beta H_\gamma$ show phase changes in this temperature region [28]. Note also that some of the chemical structures may be formed by reactions stimulated by the ionizing radiation of the electron or x-ray irradiation. In all cases the solvent/cleaning materials strongly influence the scale of the intensity steps near 200 K in the CL data (i.e. which are surface sensitive). To seek effects from Cl_2, data were recorded after immersing the samples in HCl for 15 minutes. The role of chlorine is possible because bleaching powder is frequently used to remove staining which appears during the early stages of crystal cutting. The HCl induced a different intensity change from those observed in previous measurements, but overall it displayed a broadly similar pattern.

Figure 5 indicates the temperature dependence, at four wavelengths, for a sample which had been immersed in ethanol. The results differ in detail between the various lines and can be contrasted with figure 4 in that there are narrow intensity maxima near 175 K for some lines in this example of an ethanol cleaned sample. Following ethanol cleaning there is normally an intensity increase in the interval 175–230 K for some Nd line emissions, while other lines still behave as in the original sample. A further effect is a smooth intensity increase between 130 and 170 K. Although the melting temperature of the solvents, such as ethanol, is well documented for bulk material, it is possible that for inclusions of nanoparticle size the melting or boiling points are a function of the size (as is well documented for metals). Thus if there is a nanoparticle size distribution, influenced by penetration depth into the surface via dislocation lines, then the ethanol modifications to the luminescence efficiency could exist over a wide temperature range, perhaps from 130 K to above 156 K.

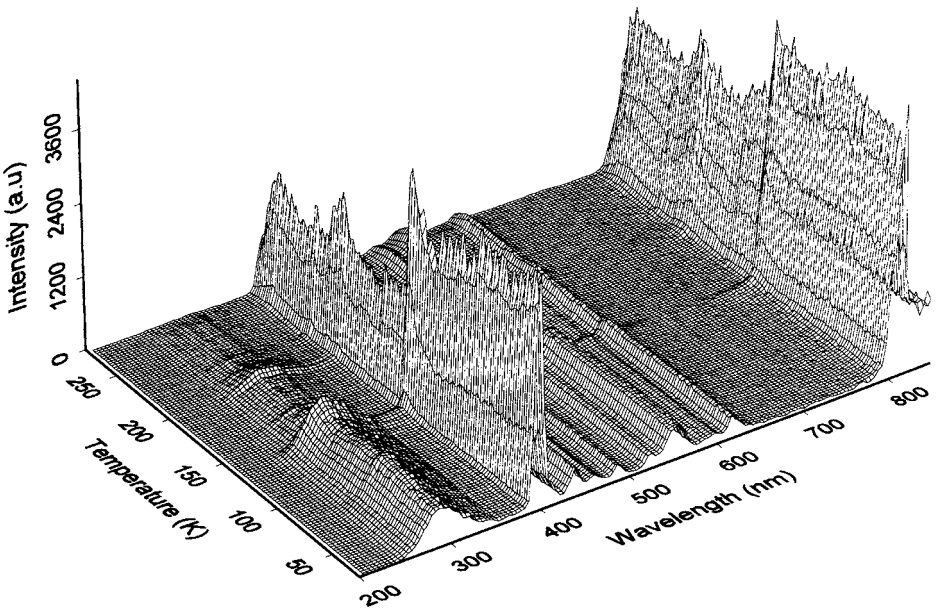

Figure 6. CL spectrum of Nd:YAG during cooling.

During cooling the excitation of luminescence differs from the previous cases since there is no previously trapped charge or modified defect sites to give additional TL type features over and above the CL temperature dependence. Indeed the CL spectra during cooling

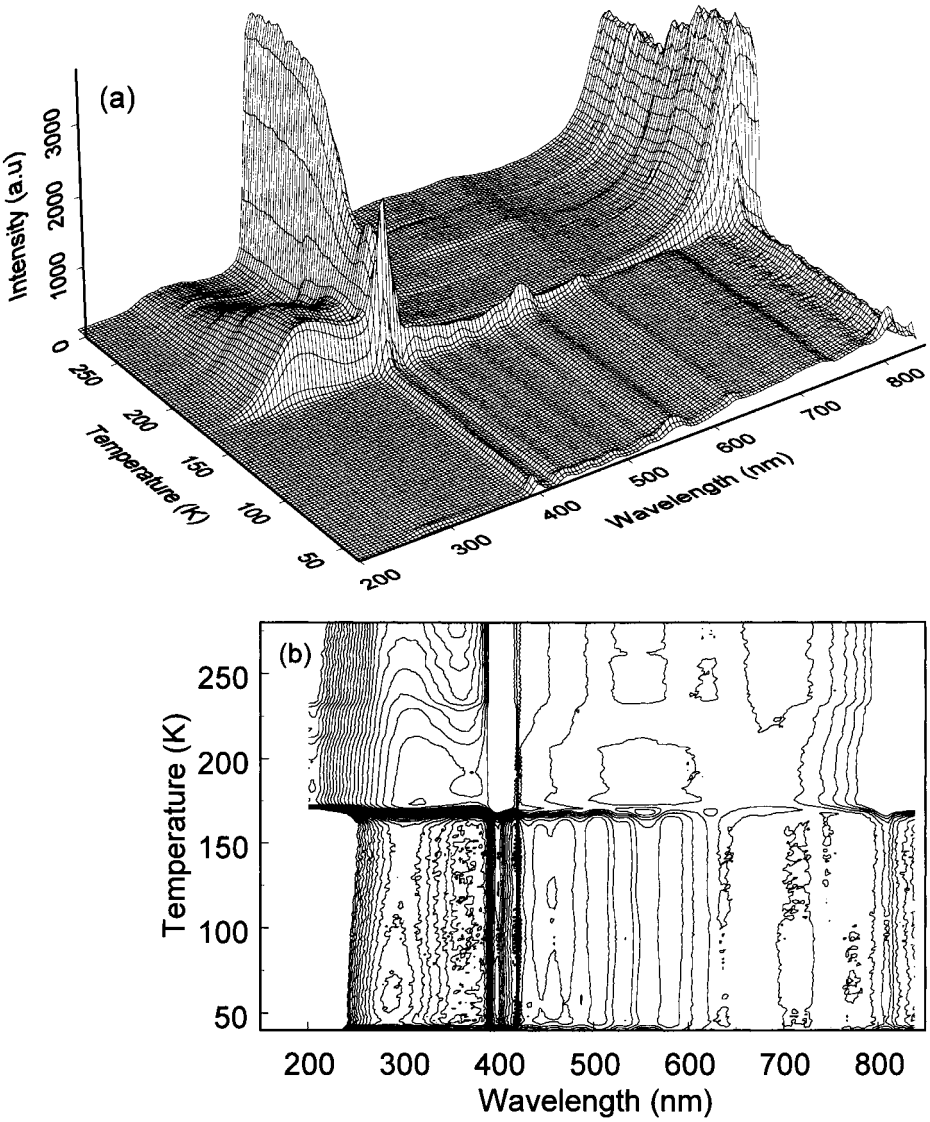

Figure 7. Isometric (a) and contour plot (b) of CL of Nd:YAG during heating.

often provided quite a different pattern from that seen during heating. One such example is presented in figure 6. Detailed inspection of such data reveals numerous discontinuous changes in intensity and wavelength displacements at the same temperatures as already noted (e.g. near 220, 200, 175 and 135 K). The main observation is that such features are not merely experimental noise as they are reproduced in different samples, albeit with variations in magnitude. It also should be recalled that CL is not a passive probe of the system as the ionization and energy deposition from the beam can alter the structure of the crystal and/or cause dissociation or release of solvents and gases trapped in the near surface region. Hence there may be differences between cooling and heating runs, or between initial and subsequent measurements.

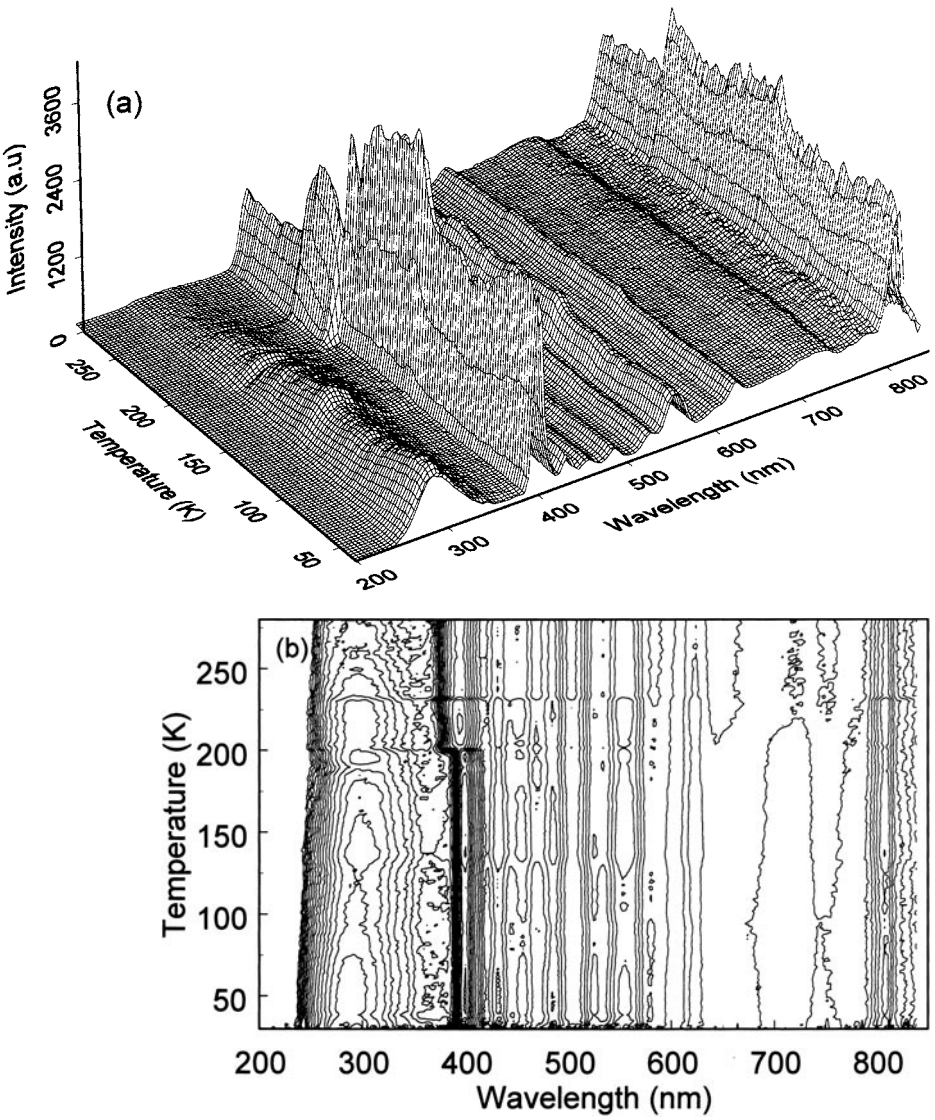

Figure 8. Isometric (a) and contour plot (b) of CL of Nd:YAG during heating, but for a different sample from that of figure 7.

Figures 7 and 8 present isometric and contour views of data taken during CL heating measurements. These figures both underline the variations which can occur between samples and the distinct changes in spectral intensity at different wavelengths. It should also be emphasized that not all the Nd lines follow the same temperature dependence with intensity. This is obvious for many lines from the original data and differences are clearly visible in figure 7 where the 400 and 800 nm regions behave very differently (see also the later figure 10). Comparisons of figures 7 and 8 reveal different intensity and temperature effects, including different temperatures for the intensity steps. Of particular note in figure 8 is an obvious step and associated wavelength shift in the 400 nm region at $\sim$200 K. Wavelength changes can be sensed to a lesser extent at the discontinuity near 230 K, where in the UV region the broad

band spectra move to shorter wavelengths for higher temperature signals. There will also be a blurring of spectral movements from the Nd lines if the material is not uniform within the volume excited by the electron beam. As noted in earlier CL studies, using depth probing by altering the electron energy, the movement of the 400 and 800 nm region signals changed with distance from the surface. The wavelength shifts were sensitive to both dislocation density and the time after polishing [2].

The features near 200 K could be consistent with CO_2 micro-bubble sublimation as the associated pressure change would modify the lattice spacing and thus shift the Nd energy levels. Indeed the scale of each of such changes will be sensitive to the particular transitions, as defined by the response of the energy levels to alterations in the crystal field. Even the direction of the change will be defined by the specific transition that generates a particular emission wavelength. In order to monitor the lattice parameter to test this proposal a small (<mm) crystal was analysed on an x-ray spectrometer. The system used has a gas controlled cooling stage and thus the lattice parameter was monitored with temperature in the region of 200 K. The sequential temperature measurements follow the cooling steps, but there may be systematic errors of several degrees in the absolute temperature which is recorded. Despite these minor temperature uncertainties the lattice parameter of the sample clearly did not follow a monotonic change with temperature and data are presented in figure 9. There is a major anomaly in the lattice parameter values over some 15 degrees around 200 K. Whilst this does not prove the presence of CO_2 it does however substantiate that the CL anomalies originate from the host YAG at this temperature. This supports a model which involves trapped or surface absorbed material. Note however that the data are from a sample obtained by grinding. It thus has a high surface to volume ratio and the response may not be identical to changes in bulk. In particular the small grain x-ray sample may expand as a result of sublimation of the CO_2 to form a high pressure gas, whereas bulk material might instead be compressed during the sublimation.

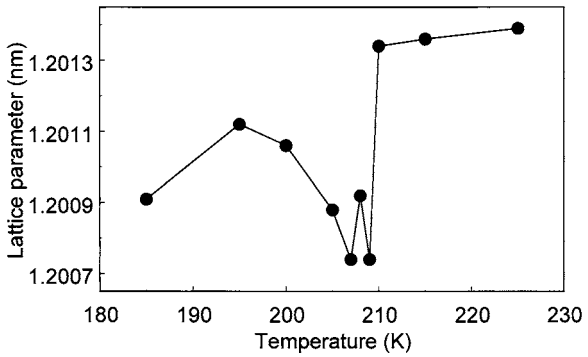

Figure 9. X-ray data of the Nd:YAG lattice parameter as a function of temperature.

Electron irradiation of insulating materials is a complex process since there is injection of charge, secondary electron emission and potential gradients defined by these effects and in the electrical conductivity of the irradiated layer. For luminescence the internal electric fields, and the possibility of electrical breakdown, could both influence the emission characteristics. The changes are also dependent on the electron penetration into the surface, and so vary with electron energy. Figure 10 gives a set of examples of energy dependence of the spectra over the range 130 to 275 K taken from the same crystal. The data underline that the spectra are very sensitive to the region within the near surface which is excited. In part the data are surprising since the higher energy electrons not only penetrate deeper into the surface but also have a

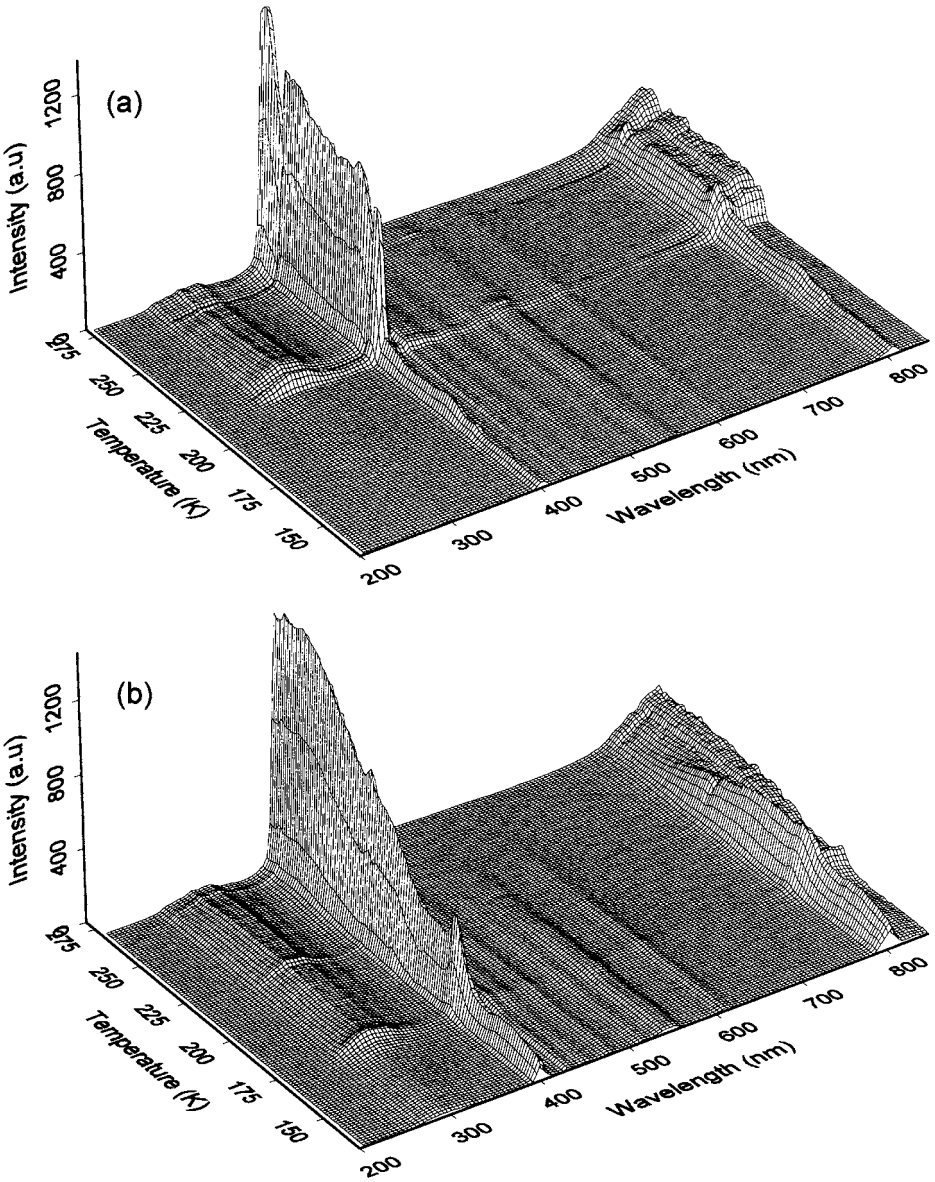

Figure 10. Cathodo-thermoluminescence (CLTL) spectra of Nd:YAG at electron energies of (a) 25 keV, (b) 20 keV, (c) 15 keV (d) 10 keV and (e) 5 keV.

higher rate of energy deposition in the shallower layers excited by low energy electrons. The first expectation is that shallow feature signals will persist in all cases and the changes will occur by the addition of signals from deeper in the layers. This set of figures contradicts this initial view.

In these examples the feature near 175 K is dominant at the lowest energy (5 keV) as a broad temperature peak with higher temperature features consistent with superposed glow peaks and a steady intensity rise. Differences appear by 10 keV with a considerable temperature narrowing of the 175 K peak plus some very slight indications of discontinuities in intensity near 200 and

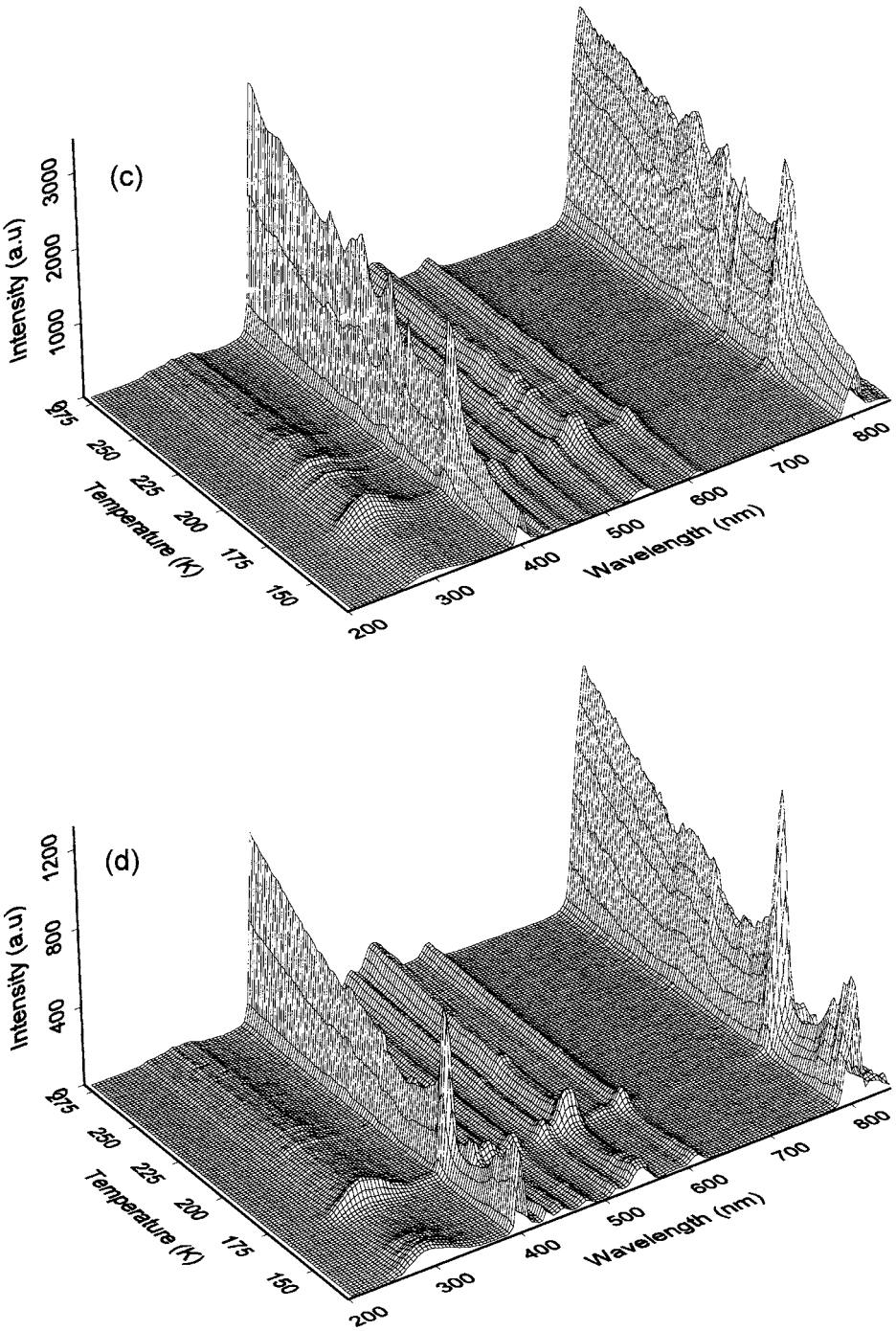

Figure 10. (Continued)

215 K. These, and other steps, start to be resolved with higher energy electrons (15 keV). By 20 keV there are major differences between behaviour near 400 and 800 nm and the 800 and 830 nm regions differ totally. Finally, by 25 keV the low temperature features are nearly all

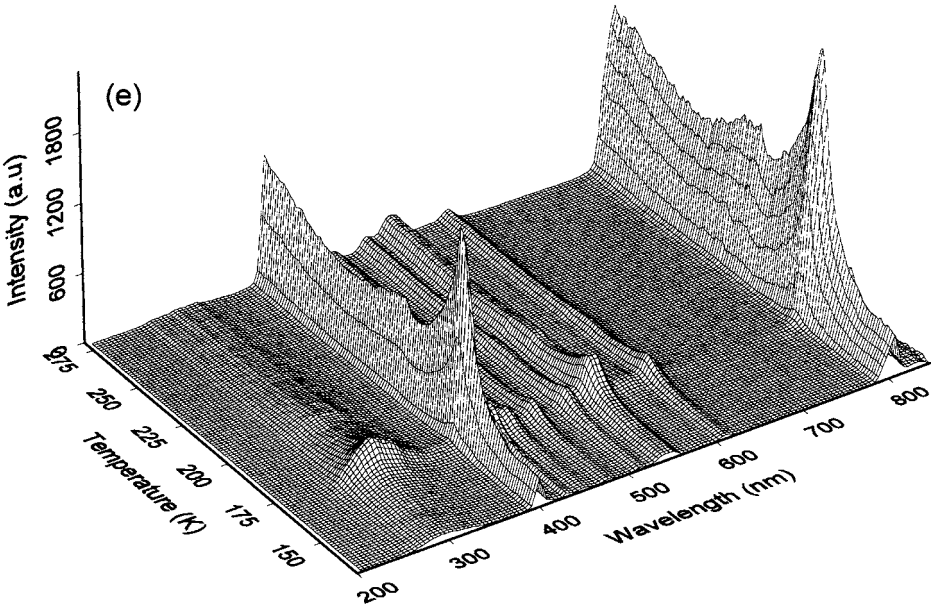

Figure 10. (Continued)

suppressed. Perhaps the zone around 220 K should be viewed as a sharp peak followed by a quenching feature, as repeated for signals near 270 K. Note overall the maximum penetration from 25 keV electrons is between one and two microns. Energy transport via exciton diffusion may of course extend the depth of the excited volume.

4. Discussion

4.1. Wavelength and depth information

There is a wealth of information obtainable from the luminescence spectra of Nd:YAG since the energies of the various Nd transitions, and their relative intensities, are sensitive to the local crystal field. Therefore any change in environment caused by the presence of dislocations, impurities, solvents or lattice parameter variations (e.g. from pressure changes) is reflected by variations in the precise position of the emission lines and their relative intensities. Unfortunately, for the current experiment, the spectrometer is not well suited to monitoring small wavelength shifts since it was designed for high collection sensitivity of transient TL spectra, and consequently it has a limited resolution ($\sim$3 nm). Nevertheless, shifts are clearly apparent, as shown visually in figures 8 and 10, and in more detailed examination of much of the other data. Changes in the environment of the near surface layers can result from the high density of dislocations formed during cutting and polishing, and as indicated in earlier work, these show spectral shifts under CL which are a function of the electron energy. This is to be expected since the lattice distortions will be greatest at the surface and for high electron energies (in this case up to 25 keV) the spectra become more typical of bulk material, and so approach the signals obtained from bulk excitation with x-rays.

As noted, the cathodoluminescence beam energy is variable from 5 to 25 keV and this enables different depth of the material to be excited. This does not imply that deconvolution of the signals as a function of depth is necessarily simplified since the rate of electron energy

deposition is not uniform with depth, but peaks at about 30% of the average electron range. Further, the luminescence efficiency from electron–hole recombination can be influenced not only by surface states, imperfections in the YAG host and dislocations, but also from longer range charge or exciton diffusion into the bulk region. Interpretation of the data of figure 10 underlines the problems involved. The lowest energies stimulate the shallowest depths of the signal and this region is most likely to have a high dislocation density from cutting and polishing. Consequently it will be most susceptible to impurity (solvent) penetration. The strong features and numerous intensity discontinuities seen at the lower energies (e.g. in figure 10(c)) may thus reflect an optimization of solvent penetration and their effects on the luminescence intensity during excitation by the electrons. Higher energy electrons will be more effective at stimulating 'bulk' material and typically will do so with a higher efficiency. One reason may be from reduced effects of quenching of the luminescence from surface states. The different electron penetration ranges will have an associated effect on the intensity of the internal electric fields generated by a combination of energy dependent secondary electron emission and charge deposition into the insulator [29]. Apparently for the present material this has the effect of quenching the surface layer signals, as is seen by the sequence of isometric plots given in figure 10.

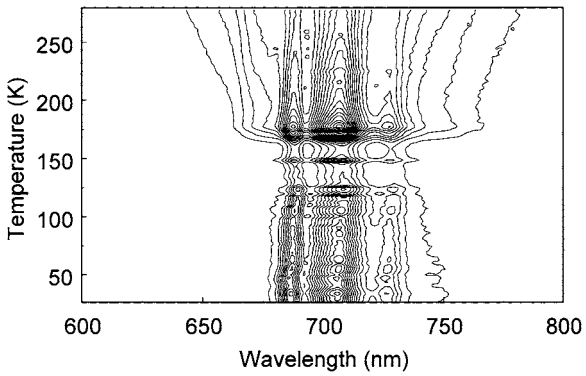

Figure 11. A contour plot of the low temperature CL intensity from a Cr:YAG crystal.

Whilst the majority of the emission lines result from the Nd ions there is also evidence in some cases, for example the high temperature TL spectra, that the samples are contaminated with traces of other rare earth elements. Tb has been clearly identified in some samples, as shown in figure 3 by the characteristic line spectra. Less clear identification can be made of some broad band emission, but a probable candidate as a trace impurity is Cr, and possibly Mn. There is broad agreement between the positions of the bands seen here and earlier published literature for these elements, as well as the current data recorded with Cr:YAG samples. (The spectra for Cr:YAG are indicated by the contour map of low temperature CL shown in figure 11.) In the TL data of Nd:YAG above room temperature there are slight differences in TL peak temperature for the various emission bands. This is to be expected if there are alternative dopants and these are not only in the luminescence recombination, but also interact with closely associated trapping sites. The initial simplistic models of TL assumed that traps and recombination sites are independent, and thus the glow peak temperatures would be insensitive to the dopants. However, current understanding of TL recognizes that the recombination centres and trapping sites are frequently sufficiently linked that they influence the binding energies (i.e. TL peak temperature) and emission energies [30, 31] so Mn and Cr variants of a TL signal will be displaced in temperature.

4.2. Separation of surface and bulk defects and the role of impurities

Even for laser quality Nd:YAG samples there are considerable problems remaining in the crystal growth. In particular these are evidenced by radial strains in the boule and subsequent surface damage associated with cutting and polishing. The former defines the regions which have a low bulk dislocation density. The surface damage is normally ignored since it represents a small fraction of the laser volume. However, the pragmatic production of working laser rods disguises the facts that surface defects exist which offer chemical penetration of solvents into the material and the original growth process may include gases trapped into the boule. Obvious candidates are from residual air in the growth furnace (e.g. N_2, O_2, CO_2, CO, Ar etc) and chemicals associated with the furnace walls and the sample preparation. Detection of such contaminants is extremely difficult and, if they do not obviously inhibit lasing, then their presence may be overlooked. The techniques of cathodoluminescence and radioluminescence conveniently offer comparative probes of the surface and bulk regions of the crystal. Additionally thermoluminescence, either after CL or RL radiation, can reveal extremely small concentrations of defect sites with either intrinsic or extrinsic origin. In all cases impurities, and intrinsic defects, influence the luminescence efficiency. The detailed spectra may aid resolution of changes which they introduce. In those cases where the solvents or trapped gases aggregate into nanoparticle size regions then their phase changes will be reflected in the luminescence intensity. This possibility has rarely been explored, even for bulk phase transitions of the host, and the potential for analysis or detection of impurities has been ignored. However, as seen here, it reveals a surprising quantity of information and indicates that gas inclusions should be considered, even for laser quality material.

The role of external contaminants which can be incorporated into the lattice via penetration along dislocation lines is interesting. All the evidence presented here suggests that such material (e.g. from HCl, ethanol, acetone etc) has a significant influence on the radiative transition probability of the Nd lines. Its role in influencing the near surface signals is consistent with the differences in intensity changes seen by contrasting the RL and CL signals, as typified by figures 4(a) and 4(b). The development of a step in intensity in the region from 175 to $\sim$220 K can also be clearly seen to be developing in the energy sequence of figure 10, and from other data not displayed here. Figure 5 showed discontinuous intensity steps as a function of wavelength, and in some cases associated with sharp peak in signal over a limited temperature range, again matched by many other examples, particularly near 175 K. Potentially such events can be linked to phase transitions within absorbed or trapped solvents. The assumption is they have penetrated the surface regions via dislocation lines caused by cutting and polishing. A strong contender for the critical temperatures observed here is based on chlorine that is present in the layer in the form of nanoparticles. Pure Cl_2 in bulk form would undergo two phase transitions, with 172 K being the cited melting point and 238 K the boiling point. The former clearly matches the nominal 175 K events seen in the Nd:YAG. Additionally, the bulk values may be modified for nanoparticle size inclusions (as for metals) and ionization driven reactions with the host lattice can form further compounds. For example Cl_2O_7, ClO_2 and Cl_2O variously have melting points of 182, 213 and 253 K respectively. Hence the presence of chlorine could generate a range of components (such as these) offering phase transitions at many of the observed key luminescence discontinuity temperatures. Alternatively there may be further impurities or compounds involved, and [28] indicates that even in a simple high temperature oxide, such as MgO, there can be a wide range of trace impurities derived from contaminants of CO_2 and H_2O. Luminescence results from radiative decay from excited states, but such states cannot be viewed in isolation from the host lattice and there are numerous examples of very long-range electron–hole or exciton luminescence, or resonant energy transfer between

impurities. These factors will explain why the presence of impurities can dominate and control the luminescence intensities of the Nd transitions. It also emphasises that the effects will differ for different transitions and why these transition probabilities will differ between the various phase or chemical associations of the impurities. Overall one can view the role of Nd as acting as a probe of the phase transitions.

In addition to Cl_2 derivatives, introduced during cleaning, there are other gaseous and liquid materials which may be added during growth, or subsequent absorption into the lattice, and/or modified by irradiation with electrons or x-rays. One such candidate is CO_2. This is a particularly interesting possibility since the material undergoes a phase transition by sublimation at 202 K for bulk CO_2, and even in a micro-bubble incorporation in the lattice may well change phase at a very similar temperature. The solid to gas phase change for a trapped volume implies a pressure rise of $\sim$1000-fold and this in turn will be transmitted into the lattice. The Nd emission will then respond with both variations in intensity and wavelength shifts induced by changes in the pressure sensitive crystal field. Figure 8 has luminescence wavelength shift evidence which would strongly support this model. Further, the x-ray lattice parameter data of figure 9, were obtained from a Nd:YAG grain of only a few hundred micron size (i.e. as a constraint of the technique used) and so are likely to be particularly sensitive to near surface effects. Figure 9 unequivocally shows a major discontinuity in lattice parameter with temperature occurs in this region. The data indicate a discontinuous expansion of the lattice near the sublimation point. For a small grain where surface effects dominate the expansion could indeed be driven by the pressure of the gas in nano-pore zones within the Nd:YAG. This is possibly the reverse of the situation within a bulk crystal where the pressure would have been expected to compress the lattice.

The differences between expansion of the surface layer and pressure driven compression of the bulk might be expected and this is probed here by the alternatives of CL and RL excitation. The lattice parameter data undergo expansion on heating through the 202 K region and CL data, as in figure 8 clearly indicate the movement of the Nd line near 400 nm to shorter wavelengths (lines near 800 nm emphasise longer wavelength signals at this point). By contrast the RLTL data for the 400 nm lines (i.e. near 393 and 398 nm) move several nm to longer wavelengths. This is consistent with pressure driven compression in the bulk and expansion at the surface.

Parallel measurements with samples of Cr:YAG reveal major differences between the CLTL and the RLTL with a variety of intensity discontinuities in the same temperature regions as for the Nd:YAG samples. A Cr:YAG example is shown in figure 11, where the contour plot indicates numerous line features. At the lower temperatures these are well matched to solid/liquid or liquid/gas phase transitions of the components of air. The effects are most dramatic for the CLTL. Although the Cr line emissions are broader features than from Nd, there are discontinuous wavelength shifts at each of these intensity steps, so again they can be interpreted in terms of phase changes of incorporated solvents and trapped gas.

5. Conclusion

Overall it is clear that the luminescence signals have revealed both bulk impurities, primarily from contaminants introduced during growth, or surface damage which has allowed the ingress of solvents and other chemicals. In both situations the contaminants appear to influence the luminescence as if they are either trapped as nanoparticles in the crystal, or within the near surface dislocation network. The particularly valuable feature of the studies with Nd doped YAG is that the rare earth lines are sharply defined and respond to changes in the local lattice symmetry and lattice parameter. Since the Nd and the Y are both tri-valent there is no additional complication from charge compensation. The unusual pattern of energy dependent CL, for the

energies used here, up to 25 keV, suggests that the surface contaminant modifications extend on the scale of at least a micron. This is consistent with penetration of solvents etc in the high dislocation density generated by cutting and polishing. A surprising feature of much of the data is that there are intensity discontinuities across the spectrum which appear relatively frequently at the same temperatures. Consistent appearances are noted near 175, 200, ∼220 and ∼270 K, as shown in many of the figures presented here, as well as the much larger quantity of data which are not displayed. The proposed explanation is that sudden discontinuities in signal intensity may well be associated with phase transitions of material, such as solvents or trapped gas in the garnet lattice. Phase transitions between solid, liquid and gas phases will modify the exciton and electron or hole mobilities, hence causing variations in the ratio of radiative to non-radiative transitions. In the case of the liquid–gas, or for CO_2 the sublimation transition at 202 K, one expects dramatic pressure changes in the lattice on generation of a gas phase. This pressure effect will either induce an extreme compression, if the gas layer is buried, or will force an expansion of the entire YAG structure for surfaces and very small crystals. This model is supported by the lattice parameter measurements of figure 9 and the significant discontinuity in emission wavelengths (as seen even in the figures for the 400 nm region in figure 8). The effects are not unique to YAG since parallel measurements of other insulating materials, to seek similar behaviour, have revealed equivalent 202 K discontinuities in the luminescence intensity in MgO. Calcium sulphate dosimeter material equally has a strong wavelength and intensity discontinuity at 202 K for the Ce and Mn emissions [19]. Additionally the sulphate material showed wavelength steps at 230 K and intensity changes near 120 K. A strong 230 K feature has been noted in CL, PL and line widths of rare earth doped $Bi_4Ge_3O_{12}$ [13, 14]. By contrast, no such features were found on recording any of the narrow line luminescence from rare earth dopants in a number of halides. Overall the suggestion is that chlorine compounds and atmospheric gases, particularly CO_2, are incorporated in the oxide and sulphate materials during growth. For CO_2 this could be in the form of a carbonate which is subsequently dissociated by the electron or x-ray irradiation.

Finally, a general inference from the study is that this type of impurity inclusion controlled process may be a much more prevalent feature, but it has been overlooked in previous studies, perhaps for experimental reasons. Equivalent intensity and wavelength movements can also be recorded during chemical changes or desorption from hydrated compounds [32].

Acknowledgments

We are extremely grateful to Dr P Hitchcock at Sussex University for x-ray measurements and the Hashemite University in Jordan and CONACYT Mexico for financial support.

References

[1] Gan Fuxi 1995 *Laser Materials* (Singapore: World Scientific) pp 163–77

[2] Peto A, Townsend P D, Hole D E and Harmer S 1997 Luminescence characterization of lattice site modifications of Nd in Nd:YAG surface layers *J. Mod. Opt.* **44** 1217–30

[3] Nunn P J T, Olivares J, Spadoni L, Townsend P D, Hole D E and Luff B J 1997 Ion beam enhanced chemical etching of Nd:YAG for optical waveguides *Nucl. Instrum. Methods* B **127/128** 507–11

[4] Vazquez G V, Rams J, Townsend P D and Hole D 1999 Improved surface quality of Nd:YAG monitored by second harmonic generation *Opt. Commun.* **167** 171–6

[5] Rowlands A P, Peto A, Townsend P D, Chandler P J, Harmer S, Hole D E, Olivares J and Randall D P 1998 Effects of surface defects on luminescence of Nd:YAG *Luminescence Materials VI* ed C R Ronda and T Welker (Pennington, NJ: Electrochemical Society) **97-29** pp 165–76

[6] Hayes W, Yamaga M, Robbins D J and Cockayne B 1980 Optical detection of EPR of recombination centres in YAG *J. Phys. C: Solid State Phys.* **13** L1085–9
[7] Robbins DJ, Cockayne B, Lent B, Duckworth C N and Glasper J L 1979 Investigation of competitive recombination in rare-earth activated garnet phosphor *Phys. Rev.* B **19** 1254–69
[8] Niklas A 1984 Thermoluminescence of YAG:Nd crystals coloured with x-rays *Appl. Phys.* B **34** 87–92
[9] Niklas A and Jelenski 1983 x-ray luminescence of YAG:Nd^{3+} *Phys. Status Solidi* a **77** 393–8
[10] Cermak K and Linka A 1981 Luminescence due to the disintegration of transient colour centres in YAG:Nd single crystals *Czech. J. Phys.* B **31** 659–63
[11] Mori K 1977 Transient colour centres caused by UV light irradiation in yttrium aluminium garnet crystals *Phys. Status Solidi* a **42** 375–84
[12] Bernhardt H J 1980 Investigation on the thermoluminescence of x-rayed YAG crystals *Phys. Status Solidi* a **61** 357–63
[13] Jazmati A K 1999 *DPhil Thesis* Sussex
[14] Jazmati A K, Townsend P D and Raymond S G 2001 Luminescence properties of rare earth doped bismuth germanate crystals and ion implanted waveguides, in preparation
[15] Niklas A 1984 Disclosure of defects in YAG crystals by the thermoluminescence method *Appl. Phys.* A **35** 249–53
[16] Brice J C 1970 Facet formation during crystal pulling *J. Cryst. Growth* **6** 205–6
[17] Garmash V M, Ermakov G A, Lyubencho V M and Filimonov A A 1986 Investigation of the influence of unstable defects on generation of laser radiation in YAG:Nd^{3+} *Sov. J. Quantum Electron.* **16** 558–60
[18] Rotman S R 1997 The effect of defects on inorganic luminescent materials *Wide-Gap Luminescent Materials* ed S R Rotman (Boston: Kluwer) ch 2, pp 139–90
[19] Maghrabi M, Karali T, Townsend P D and Lakshmanan A R 2000 Luminescence spectra of $CaSO_4$ with Ce, Dy, Mn and Ag codopants *J. Phys. D: Appl. Phys.* **33** 477–84
[20] Rowlands A P, Karali T, Terrones M, Grobert N, Townsend P D and Kordatos K 2000 Cathodoluminescence of fullerene C_{60} *J. Phys.: Condens. Matter* **12** 7869–78
[21] Garmash V M, Ermakov G A, Lyubencho V M and Filimonov A A 1986 Investigation of thermoluminescence of Nd doped YAG crystals *Opt. Spectrosc.* **61** 337–9
[22] Wall W A, Karpick J T and Bartolo D I 1971 Temperature dependence of the vibronic spectrum and fluorescence lifetime of YAG:Cr^{3+} *J. Phys. C: Solid State Phys.* **4** 3258–65
[23] Bernhardt H J 1976 The manganese-induced O^- centres in yttrium aluminium garnet *Phys. Status Solidi* a **37** 445–8
[24] Henderson B, Gallagher H G, Han T P J and Scott M A 2000 Optical spectroscopy and optimal crystal growth of some Cr^{4+} doped garnets *J. Phys.: Condens. Matter* **12** 1927–38
[25] Townsend P D, Rowlands A P and Corradi G 1997 Thermoluminescence during a phase transition *Radiat. Meas.* **27** 31–6
[26] Yang B, Townsend P D and Maghrabi M 2001 Optical detection of phase transitions in potassium niobate *J. Mod. Opt.* **48** 319–31
[27] Arsenev P A, Vakhidov S A and Ibragimova E M 1974 Some structural defects in $YAlO_3$:Nd single crystals *Phys. Status Solidi* a **21** K35–8
[28] Freund F, Gupta A D and Kumar D 1999 Carboxylic and dicarboxylic acids extracted from crushed magnesium oxide single crystals *Origins Life Evolution Biosphere* **29** 489–509
[29] Cazaux J 1986 Some considerations on the electric-field induced in insulators by electron bombardment *J. Appl. Phys.* **59** 1418–30
[30] McKeever S W S, Moscovitch M and Townsend P D 1995 *Thermoluminescence Dosimetry Materials: Properties and Uses* (Ashford: Nuclear Technology)
[31] Townsend P D, Jazmati A K, Karali T, Maghrabi M, Raymond S G and Yang B 2001 Rare earth size effects on thermoluminescence and second harmonic generation *J. Phys.: Condens. Matter* **13** 2211–24
[32] Ramachandran V 2001 Luminescence changes during heating of silica gel, in preparation